Molecular Biology of the Cell
Vol. 20, 1269–1279, March 1, 2009

The Role of FilGAP-Filamin A Interactions in Mechanoprotection

Yulia Shifrin,* Pamela D. Arora,* Yasutaka Ohta,† David A. Calderwood,‡ and Christopher A. McCulloch*

*CIHR Group in Matrix Dynamics, University of Toronto, Toronto, Ontario M5S 3E2, Canada; †Department of Biosciences, School of Science, Kitasato University, Sagamihara Kanagawa 228-8555, Japan; and ‡Department of Pharmacology and Interdepartmental Program in Vascular Biology and Transplantation, Yale University School of Medicine, New Haven, CT 06520

Submitted August 26, 2008; Revised December 19, 2008; Accepted January 6, 2009
Monitoring Editor: Yu-Li Wang

Cells in mechanically active environments are subjected to high-amplitude exogenous forces that can lead to cell death. Filamin A (FLNa) may protect cells from mechanically induced death by mechanisms that are not yet defined. We found that mechanical forces applied through integrins enhanced Rac-mediated lamellae formation in FLNa-null but not FLNa-expressing cells. Suppression of force-induced lamella formation was mediated by repeat 23 of FLNa, which also binds FilGAP, a recently discovered Rac GTPase-activating protein (GAP). We found that FilGAP is targeted to sites of force transfer by FLNa. This force-induced redistribution of FilGAP was essential for the suppression of Rac activity and lamellae formation in cells treated with tensile forces. Depletion of FilGAP by small interfering RNA, inhibition of FilGAP activity by dominant-negative mutation or deletion of its FLNa-binding domain, all resulted in a dramatic force-induced increase of the percentage of annexin-V–positive cells. FilGAP therefore plays a role in protecting cells against force-induced apoptosis, and this function is mediated by FLNa.

INTRODUCTION

Mechanical forces are important physiological regulators, from the level of molecules to the whole organism. In many types of mechanically loaded tissues, supranormal force levels increase the incidence of cell death (Cheng *et al*., 1995; Edwards *et al*., 2000; Kobayashi *et al*., 2000) and may also contribute to pathological states such as cardiac hypertrophy (Sadoshima and Izumo, 1997) and atherosclerosis (Thubrikar and Robicsek, 1995). Cells that are subjected to high-amplitude mechanical forces in vivo undergo dramatic internal structural changes (Malek and Izumo, 1996) that enable them to maintain membrane integrity, shape, and adhesion to extracellular matrix molecules (Glogauer *et al*., 1997; McNeil and Steinhardt, 1997). The failure to adapt to applied mechanical stimuli leads to the tissue destruction and loss of homeostasis observed in diseases including osteoarthritis (Lin *et al*., 2004), lung injury (Lionetti *et al*., 2005), and heart failure (Cheng *et al*., 1995).

Cells may be able to sense and adapt to environmental tension, in part through cytoskeletal adaptations. One suggested mechanism of direct transfer of forces from the extracellular matrix to the actin cytoskeleton involves integrins as mechanotransducers (Huang and Ingber, 1999; Katsumi *et al*., 2004; (Chen *et al*., 2004). Forces applied through integrins subsequently lead to reorganization of subcortical actin and alteration of cellular gene expression (Shyy and Chien, 1997; Chien *et al*., 1998; Critchley, 2000). Filamin A (FLNa) is an example of a cytoskeletal gene that is induced by mechanical forces applied through β1 integrins (D'Addario *et al*., 2001, 2002). FLNa belongs to a family of high-molecular mass cytoskeletal proteins that cross-link actin filaments and link actin networks to cell membranes (Cunningham *et al*., 1992; Stossel *et al*., 2001; van der Flier and Sonnenberg, 2001). FLNa has been implicated in mechanoprotection (Glogauer and Ferrier, 1998) and increased FLNa production by high-amplitude tensile forces facilitates cell survival, in part by mechanical stabilization of cortical actin and prevention of force-induced cell depolarization (Kainulainen *et al*., 2002).

In addition to binding and cross-linking actin filaments, FLNa interacts with a diverse array of proteins that impact a wide range of cellular functions (Feng and Walsh, 2004; Popowicz *et al*., 2006). Among FLNa-binding proteins are actin-regulating RhoGTPases, including RhoA, Rac, Cdc42 (Marti *et al*., 1997), and RalA (Ohta *et al*., 1999), as well as their downstream effectors (Vadlamudi *et al*., 2002; Ueda *et al*., 2003). FLNa also binds TRIO and Lbc, guanine nucleotide-exchange factors (GEFs) for Rac and Rho, respectively (Bellanger *et al*., 2000; Pi *et al*., 2002), and a recently discovered GTPase-activating protein (GAP) for Rac (Ohta *et al*., 2006). Notably, small GTPases have been implicated in many aspects of cell physiology, including proliferation, differentiation, cytoskeletal organization, vesicle trafficking, nucleocytoplasmic transport, and gene expression (Hall, 1998; Takai *et al*., 2001; Wennerberg *et al*., 2005). Small GTPases have also emerged as important coordinators of cytoskeletal rearrangements and gene expression in response to exogenous force (Tzima, 2006). FLNa therefore may play an important role in signaling through small GTPases to effect changes in the organization of the actin cytoskeleton.

This article was published online ahead of print in *MBC in Press* (http://www.molbiolcell.org/cgi/doi/10.1091/mbc.E08–08–0872) on January 14, 2009.

Address correspondence to: Yulia Shifrin (yulia.shifrin@utoronto.ca).

Abbreviations used: FLNa, filamin A; FilGAP, filamin A-associated RhoGAP; siRNA, small interfering RNA.

In this article, we provide evidence that FilGAP, a novel Rac GAP, is targeted to sites of force transfer by FLNa. This force-induced redistribution of FilGAP is essential for suppressing Rac activity and lamellae formation in cells challenged by tensile forces. The FilGAP–FLNa interaction in response to mechanical stimuli plays a mechanoprotective role, contributing to the ability of cells to resist force-induced apoptosis.

MATERIALS AND METHODS

Antibodies

Monoclonal antibodies were purchased from Sigma-Aldrich (St. Louis, MO) (vinculin and β-actin), Millipore (Billerica, MA) (Rac and Rho), Roche Applied Science (Indianapolis, IN) (hemagglutinin [HA]), Serotec (Oxford, United Kingdom) (FLNa), Millipore (cortactin), BD Biosciences Pharmingen (integrin β1 chain and KMI6), and Beckman Coulter (Mississauga, ON, Canada) (β1 integrin and 4B4-RD1). Polyclonal antibody to FilGAP was a generous gift of T. Stossel (Brigham and Women's Hospital, Boston, MA). Secondary Cy3-conjugated goat anti-mouse antibody and (fluorescein isothiocyanate [FITC])-conjugated goat anti-mouse antibody were purchased from Sigma-Aldrich. Anti-mouse or anti-rabbit horseradish peroxidase (HRP)-linked secondary antibodies were purchased from GE Healthcare (Little Chalfont, Buckinghamshire, United Kingdom).

Cell Culture and Transfection

The human melanoma cell lines M2 and A7 were grown in minimum essential medium supplemented with 8% newborn calf serum and 2% fetal calf serum and antibiotics (0.17% wt/vol penicillin V, 0.1% gentamicin sulfate, and 0.01% μg/ml amphotericin). Human embryonic kidney (HEK) 293 cells were grown at 37°C in DMEM supplemented with 10% fetal bovine serum and antibiotics. NIH 3T3 cells were grown in DMEM supplemented with 10% calf serum and antibiotics. NIH 3T3 cells stably transfected with a short hairpin RNA (shRNA) against FLNa (Kiema *et al*., 2006) were grown in the presence of in puromycin (1 μg/ml). For transfection, cells were trypsinized, plated on fibronectin-coated (10 μg/ml; Sigma-Aldrich) coverslips or 100-mm dishes and immediately transfected using FuGENE6 transfection reagent, as described by the manufacturer (Roche Applied Science). To generate stably transfected cells, selection media were applied after 48 h of transfection. Stable colonies were expanded and screened by immunoblot using anti-FLNa antibody.

Preparation of Coated Beads and Force Application

Tensile mechanical forces were applied to cells using a previously described model system (Glogauer *et al*., 1995; Glogauer and Ferrier, 1998). Magnetite microparticles (Fe_3O_4; Sigma-Aldrich) were used for isolation of bead-associated proteins and for Rac-/Rho-activation assays. Superparamagnetic microspheres (Bangs Laboratories, Fishers, IN) were used for immunofluorescence microscopy. Beads were incubated with purified collagen (Vitrogen 100, 1 mg/ml; Cohesion Technologies, Palo Alto, CA), neutralized to pH 7.4, or with bovine serum albumin (BSA, 1.3 mg/ml; Sigma-Aldrich) and rinsed with phosphate-buffered saline (PBS). Beads were incubated with cells in a serum-free medium for 15 min to prevent bead internalization. Excess nonadherent beads were removed by washing and the cells were supplemented with fresh serum-containing medium. A ceramic permanent magnet (Jobmaster, Mississauga, ON, Canada) was used to generate perpendicular, tensile forces on beads attached to the dorsal surface of cells. The pole face was oriented parallel with the culture dish surface at a distance of 20 or 40 mm from the surface, depending on the experiment. At these distances, single cells would be expected to experience tensile forces of 0.6 and 0.3 Pa, respectively (Glogauer and Ferrier, 1998).

Confocal Microscopy and Flow Cytometry

Cells plated on fibronectin-coated coverslips were incubated with collagen- or BSA-coated magnetite beads and subjected to force as described above. Cells were fixed with 3% formaldehyde in phosphate-buffered saline, permeabilized with 0.2% Triton X-100 (Sigma-Aldrich), and stained with the primary antibody followed by secondary antibody, as described for each individual experiment. For actin localization cells were stained with FITC- or rhodamine-phalloidin (Sigma-Aldrich). For quantification of lamellopodia, cells were incubated with anti-cortactin antibody, rinsed in PBS, and incubated with Cy3-conjugated goat anti-mouse antibody. For localization of HA-tagged FilGAP, cells were incubated with monoclonal anti-HA antibody, followed by Cy3-conjugated goat anti-mouse antibody. Cells were rinsed, coverslips were mounted on glass slides with Immuno-fluor mounting solution (10 μl; MP Biomedicals, Irvine, CA) and examined by confocal microscopy (TCS, 40× oil immersion lens; Leica, Heidelberg, Germany).

For flow cytometry analyses, cells were stained with antibodies to mouse or human β1 integrins for 1 h at 37°C and analyzed on a Coulter Altra flow cytometer (Beckman Coulter). For all flow cytometry analyses, at least 1×10^5 cells were assessed in each sample.

Rac and Rho Activation

To determine guanosine triphosphate (GTP) loading of Rac and Rho in vivo, HEK293 cells were grown on 100-cm dishes and transiently transfected with relevant plasmids for 48 h. After treatments indicated for each individual experiment, cells were washed in ice-cold PBS and lysed in radioimmunoprecipitation assay buffer (20 mM Tris-HCl, pH 7.5, 120 mM NaCl, 1% Triton X-100, 0.5% sodium deoxycholate, 0.1% SDS, 10 mM $MgCl_2$, 0.2 M phenylmethylsulfonyl fluoride, 10 μg/ml aprotinin, and 10 μg/ml leupeptin) at 4°C. The cell lysates were cleared, and supernatants were sampled for the determination of total GTPases or incubated with glutathione transferase (GST) fusion proteins (Millipore) corresponding to the p21-binding domain (PBD, expressed in *Escherichia coli* and bound to glutathione agarose) or the rhotekin-binding domain (RBD, expressed in *E. coli* and bound to glutathione agarose). The beads were washed and boiled in 2× Laemlli buffer. Samples were separated on 10% SDS-polyacrylamide gel electrophoresis (PAGE) gels, transferred to nitrocellulose membranes, and probed with Rac and Rho antibodies. Supernatants were also run on SDS-PAGE gels and immunoblotted for total Rac and Rho.

Immunoblotting

Cells were lysed and cellular proteins were separated by SDS-PAGE and transferred to nitrocellulose (Whatman Schleicher and Schuell, Keene, NH). The percentage of the gel varied from 8 to 15%, depending on the size of the analyzed protein. Protein concentrations of cell lysates were determined using the bicinchoninic acid protein assay kit (Pierce Chemical, Rockford, IL). Equal amounts of protein were loaded on individual lanes and nitrocellulose membranes were probed for the indicated antibody: FLNa, β-actin, FilGAP, HA, and vinculin, followed by incubation with anti-mouse or anti-rabbit HRP-linked secondary antibody. Chemiluminescent detection was performed according to the manufacturer's instructions (ECL; GE Healthcare). The radiographic films were exposed for standardized times by using conventional methods.

Extraction of Bead-Associated Proteins

Bead-associated adhesion complexes were isolated and immunoblotted as described previously (Plopper and Ingber, 1993). Briefly, after designated incubation times, cells and attached collagen-coated magnetic beads were collected by scraping into ice-cold extraction buffer [CSK-EB: 0.5% Triton X-100, 50 nM NaCl, 300 mM sucrose, 3 mM $MgCl_2$, 2 mM 4-(2-aminoethyl) benzenesulfonyl fluoride, 1 mM EDTA, 30 μM bestatin, 14 μM E-64, 1 μM leupeptin, 0.3 μM aprotinin, and 10 mM piperazine-*N*,*N*′-bis(2-ethanesulfonic acid), pH 6.8]. Beads were pelleted using a side-pull magnetic isolation apparatus (Dynal, Lake Placid, NY), and supernatants were collected. Isolated beads were resuspended, sonicated, homogenized, and washed three times in extraction buffer before PAGE and Western blot analysis.

RNA Interference Experiments

For depleting endogenous FLNa, cells were transfected with the interference vector pPUR/U6/FLNa (Meng *et al*., 2004) (a generous gift from Z. Shen, University of New Mexico, Albuquerque, NM) by using FuGENE6 transfection reagent. Empty vector was used as a negative control. At 2 d after transfection, 5 μg/ml puromycin was added to the medium to establish stably transfected cell line. Levels of FLNa in isolated clones were analyzed by immunoblotting with anti-FLNa antibody. For depleting the endogenous FilGAP, siRNA oligonucleotides were purchased from QIAGEN (Valencia, CA). The targeting sequence of *FilGAP* was 5′-ACCGAGAGAGGAAACACAATA-3′ (nucleotides 2215–2235), as described previously (Ohta *et al*., 2006). The transfection efficiency of siRNA was determined by immunofluorescence microscopy by using Alexa488-labeled *FilGAP* siRNA. HEK293, NIH 3T3, M2, or A7 cells were transfected with 200 pmol of *FilGAP* or control siRNA oligonucleotides by using Oligofectamine reagent (Invitrogen); 48 h after transfection, cells were lysed and the level of FilGAP was measured by immunoblotting using polyclonal anti-FilGAP antibodies.

Plasmids and Mutant FLNa and FilGAP Constructs

Human filamin A constructs were produced as follows. First, pcDNA3 vector carrying c-Myc tagged full length FLNa cDNA (Kainulainen *et al*., 2002) was excised with HindIII and BamHI restriction endonucleases (New England BioLabs, Ispwich, MA) and subsequently cloned into the DsRed2-C1 vector (Clontech, Mountain View, CA). Next, we used previously described single-step single-primer site-directed mutagenesis technique (Makarova *et al*., 2000) to introduce five silent mutations into the siRNA targeting sequence of the filamin A gene (nucleotides 3246-3066) changing it into GGGCCGATAATAGCGTAGTTC. Briefly, a single mutagenic primer (5′-TGGAGCCAGGCCTGGGGGCCGATAATAGCGTAGTTCGCTTCCTGC-3′) was designed. The polymerase chain reaction (PCR) mutagenesis reaction was performed in a reaction volume of 25 μl that included 1 μl of DsRed2-C1 FLNa template isolated using QIAprep Spin miniprep kit (QIAGEN), 200 nM primer, 200 μM dNTPs, 10% dimethyl sulfoxide, and 1.25U *Pfu* enzyme in 1× *Pfu* DNA polymerase reaction buffer (Invitrogen). A preliminary step of denaturation at 95°C for 3 min was followed by 18 cycles of PCR. These PCR cycles consisted of 15 s of denaturation at 95°C, 1 min of annealing at 56°C, and 15 min of

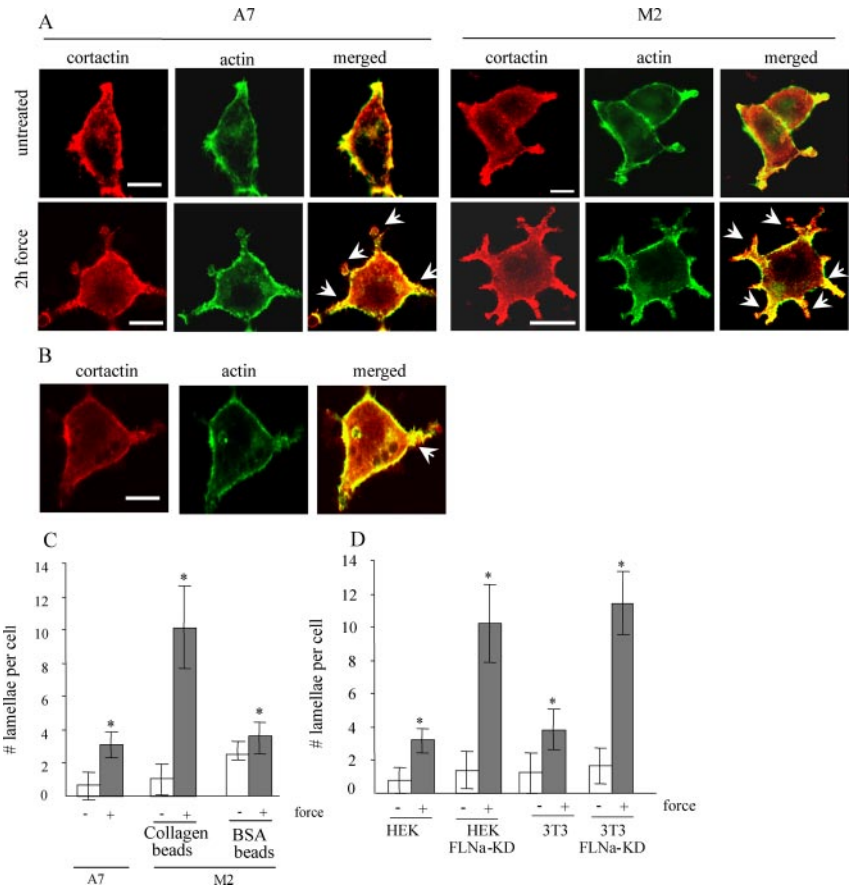

Figure 1. Enhanced lamellae formation in filamin A-deficient cells. (A) FLNa-repleted A7 or FLNa-deficient M2 cells were grown on fibronectin-coated glass coverslips, incubated with collagen-coated ferromagnetic beads, and either left untreated or subjected to mechanical force. Cells were stained with FITC-phalloidin for actin filaments and with cortactin antibody for lamellipodia (red). Arrowheads indicate lamellipodia. (B) β1 Integrins are required for force-induced lamellae formation. M2 cells were incubated with BSA- or collagen-coated beads and treated as in A. Lamellipodia are indicated by arrowheads. Bar, 10 μm. (C) Quantification of lamellipodia on individual cells treated in A and B. The data are presented as the mean ± SE of 10 cells for each column. (D) Control and FLNa-knockdown NIH 3T3 fibroblasts were incubated with collagen beads and left untreated or subjected to force. Lamellopidia in individual cells were counted and the data are presented as the mean ± SE of five cells for each column. *$p < 0.00001$ versus respective untreated control.

extension at 68°C. Finally, the PCR product was treated with DpnI restriction endonuclease and transformed into XL1-Blue supercompetent cells (Stratagene, La Jolla, CA). Mutations were verified by sequencing performed at the DNA Sequencing Facility, Center for Applied Genomics (Hospital for Sick Children, Toronto, ON, Canada). The final mutant was used as a template to generate a deletion of the 23rd terminal repeat of the FLNa. A single mutagenic primer (5′-AACCCAGCTGAGTTCGTCGTGAACAGCTTCACAGTAGACTGCAGC-3′) was designed. The first 24 nucleotides of the primer corresponded to the sequence immediately upstream of the 23 repeat (nucleotides 7336-7359 of the coding region of the filamin A gene), and the last 21 nucleotides corresponded to the sequence immediately downstream of the 23 repeat (nucleotides 7729-7749 of the coding region of the filamin A gene). The deletion was verified by sequencing. HA-tagged FilGAP mutant lacking the coiled-coil domain (FilGAP$^{\Delta CC}$) was generated as described previously (Ohta *et al.*, 2006). Briefly, the FilGAP–HA-pCMV5 vector was digested with BamHI and self-ligated. The deletion was verified by diagnostic restriction endonuclease cleavage. Full-length HA-tagged FilGAP construct and HA-tagged dominant negative FilGAP mutant lacking the GAP domain (FilGAP$^{\Delta GAP}$) were a kind gift of T. Stossel (Harvard Medical School, Boston, MA). pEGFP-C1 FilGAP construct was a kind gift of M. Glogauer (University of Toronto, Toronto, ON, Canada). Next, five silent mutations were introduced to a siRNA targeting sequence of all FilGAP constructs changing it into *ACGGAGACGGGTAACACTATT* by single-step single-primer site-directed mutagenesis using mutagenic primer 5′-GAACCCAGGAGAACGGAGACGGGTAACACTATTTGGATTCAGTGA-3′. All mutations were verified by sequencing.

Identification and Quantification of Early Force-induced Cell Death

Annexin-V is a phospholipid-binding protein with a high affinity for phosphatidylserine (PS). Detection of cell-surface PS with annexin-V thus serves as a marker for an early stage of apoptosis (van den Eijnde *et al.*, 1997). After force application, cells were vitally stained with propidium iodide (PI) and annexin-V by using the Annexin-V-Fluos staining kit (Roche Applied Science) and examined with a fluorescence microscope at 250×. Alternatively, after fixation and permeabilization cells were counterstained with 4,6-diamidino-2-phenylindole (DAPI). The number of annexin-V–stained cells and the total number of cells were counted in three different sampling grids for each sample to yield the percentage of apoptotic cells. Data from three separate areas were averaged for each sample.

Statistical Analysis

For all studies, experiments were repeated at least three times. For quantitative data, means and standard deviations were computed. When appropriate, sample comparisons were analyzed by Student's unpaired *t* test and statistical significance set at $p < 0.05$.

RESULTS

FLNa Suppresses Force-induced Lamellae Formation and Rac Activation

We investigated the role of FLNa in stabilizing cell actin cytoskeleton in response to mechanical forces. Filamin-deficient M2 melanoma cells and FLNa-expressing A7 cells were incubated with collagen-coated ferromagnetic beads and subjected to mechanical forces (pole face at 20 mm from the culture dish surface). Care was taken to maintain equal amount of bead loading between cells. We estimated the number of lamellipodia in cells with actin filament staining (with phalloidin) and with immunostaining for cortactin. This actin-binding protein is activated by external stimuli to promote assembly and rearrangement of actin filaments and is especially abundant in the subcortex and in lamellipodia (Weaver *et al.*, 2001; Weed and Parsons, 2001). In M2 cells, treatment with force strongly stimulated the formation of multiple lamellae (an average of 10.1 lamellae/cell). By contrast, A7 cells subjected to force formed very few lamellae (an average of 3.1/cell) (Figure 1, A and C). This response was not detected when force was applied to cells through beads coated with BSA. In M2 cells, force transmitted

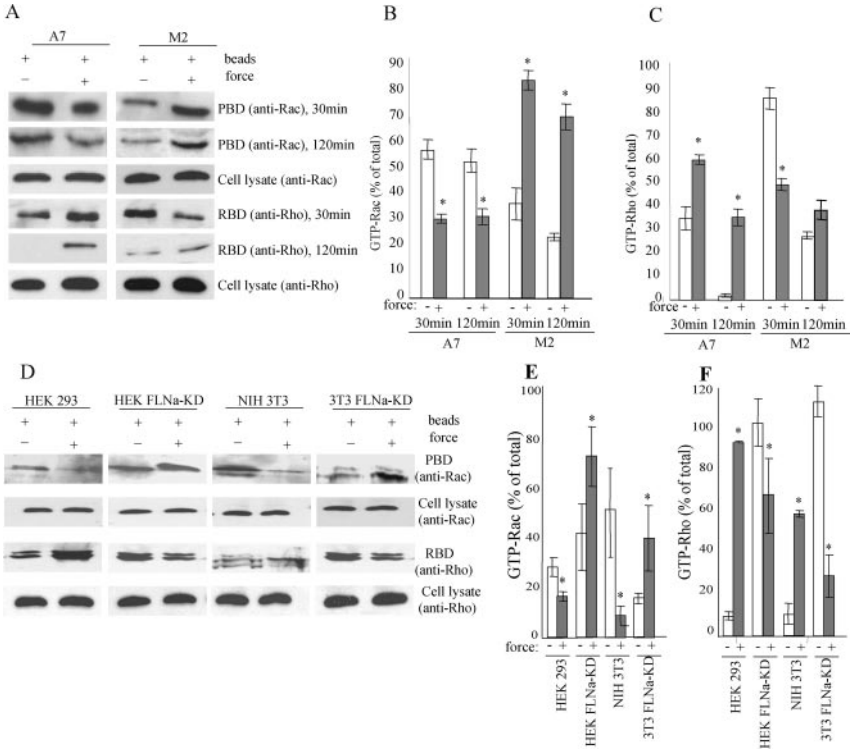

Figure 2. Force-induced Rac activation. (A) FLNa-repleted A7 and FLNa-deficient M2 cells were subjected to mechanical force for 30 min and 2 h as described previously. Cell extracts were then incubated with GST-PBD or GST-RBD immobilized on glutathione-Sepharose beads. The amounts of Rac and Rho in cell lysates before pull-down, GST-PBD bound Rac, and GST-RBD bound Rho were detected by immunoblot. Intensities of GST-PBD bound Rac bands (B) and Rho bands (C) were measured using ImageJ densitometry software. Numbers represent ratios relative to the levels of Rac and Rho in cell lysates before pull-down and are expressed as the means and SDs of three independent experiments. *$p < 0.05$ versus respective untreated control (D) Control HEK, FLNa-knockdown HEK, control NIH 3T3, and FLNa-knockdown 3T3 were subjected to mechanical force for 2 h and treated as described in A. The amounts of GST-PBD–bound Rac, GST-RBD–bound Rho, and Rac and Rho in cell lysates before pull-down were detected by immunoblot and quantified using ImageJ software. Numbers represent ratios relative to the levels of Rac and Rho in cell lysates before pull-down and are expressed as the means and SDs of three independent experiments. *$p < 0.03$ versus respective untreated control.

through BSA-coated beads resulted in an average of 3.8 lamellae per cell (Figure 1, B and C).

We investigated further the response of cells to mechanical stimuli with the use of FLNa-knock down HEK cells (HEK FLNa-KD), generated by shRNA targeting with RNA interference vector pPUR/U6 (Meng *et al*., 2004), and with NIH 3T3 cells where endogenous FLNa was stably depleted using shRNA. Control HEK cells, HEK FLNa-KD cells, control NIH 3T3, and 3T3 FLNa-KD were incubated with collagen-coated ferromagnetic beads and subjected to mechanical force (~0.6 pN/μm^2). In FLNa-deficient HEK FLNa-KD and 3T3 FLNa-KD cells, treatment with force strongly stimulated the formation of multiple lamellae (an average of 10.2 and 11.4 lamellae/cell, respectively) comparing with an average of 3.1 and 3.8 lamellae per cell in control HEK and 3T3 cells, respectively (Figure 1D).

Because stress fibers and lamellipodia formation are thought to be mediated by Rho and Rac activity, respectively (Hall 1998), we applied tensile forces to bead-loaded M2 and A7 cells for 30 min or 2 h, and measured the relative abundance of active Rac1 and Rho (Figure 2A). Both short (30-min) and prolonged (2-h) exposure to force promoted significant increases in the level of GTP-Rac in filamin-deficient M2 cells (2.3-fold after 30 min and threefold after 2 h of force application) (Figure 2B). In contrast, FLNa-expressing A7 cells exhibited 1.9- and 1.6-fold force-induced decreases of Rac activity after exposure to force for 30 min and 2 h, respectively (Figure 2B). Short (30-min) exposures to force led to 1.9-fold decreases in levels of active Rho in M2 cells comparing with 1.7-fold increases in A7 cells (Figure 2C). After 2-h force application, the levels of active Rho in A7 increased dramatically (34-fold) compared with only a 1.8-fold increase in M2 cells (Figure 2C). Similarly, force-challenged HEK FLNa-KD and 3T3 FLNa-KD cells lacking FLNa exhibited a 1.6- and 2.5-fold increase in the level of GTP-Rac, respectively. Conversely, FLNa-expressing HEK and NIH 3T3 cells exhibited 1.7- and 6.3-fold force-induced decreases of Rac activity, respectively (Figure 2, D and E). The levels of active Rho in HEK and NIH 3T3 cells increased 9.7- and 5.7-fold, respectively, after treatment with force, whereas HEK FLNa-KD and 3T3 FLNa-KD cells exhibited 1.5- and 3.8-fold force-induced decreases in Rho activity (Figure 2, D and F). Together, these data demonstrate that mechanical force, applied through integrins, leads to enhanced lamellae protrusion and Rac activation in FLNa-deficient cells and to enhanced Rho activation in FLNa-expressing cells.

Previous studies showed that collagen-coated magnetite beads attach to cells via β1 integrins (Glogauer *et al*., 1997). Conceivably, the observed differences in cellular responses to force between the various cell types used here were due to variations in the cell surface abundance of β1 integrins. Accordingly, nonpermeabilized HEK, HEK FLNa-KD, NIH 3T3, 3T3 FLNa-KD, M2, and A7 cells were stained with antibodies against the β1 integrin; fluorescence intensity was estimated by flow cytometry. The mean fluorescence intensities $\pm$standard deviations were: 3.4 $\pm$ 1.2 (HEK cells), 4.1 $\pm$ 2 (HEK FLNa-KD cells), 1.2 $\pm$ 1 (NIH 3T3 cells), 1.3 $\pm$ 1 (FLNa-KD cells), 3.5 $\pm$ 2 (M2 cells) and 5.2 $\pm$ 3 (A7 cells). These data demonstrate no statistically significant differences ($p > 0.2$) of cell surface β1 integrins for the relevant pairs of cells.

We examined tensile force-induced cellular deformation in FLNa-expressing and FLNa-deficient cells. M2 and A7 cells were loaded with collagen-coated ferromagnetic beads (Figure 3A) and subjected to mechanical force of different magnitudes by placing the magnet at 20 or 40 mm from the pole face. We evaluated changes in vertical deformation and Rac activity (Figure 3, B and C). At the lower force level both M2 and A7 cells exhibited a similar amount of deformation (Figure 3B). However, in M2 cells we observed a 1.8-fold increase of Rac activity, whereas the levels of GTP-Rac in A7 cells decreased twofold. At the higher force level (20 mm from the pole face), the deformation of M2 cells increased 2.3-fold and was accompanied by an overall 1.6-fold increase

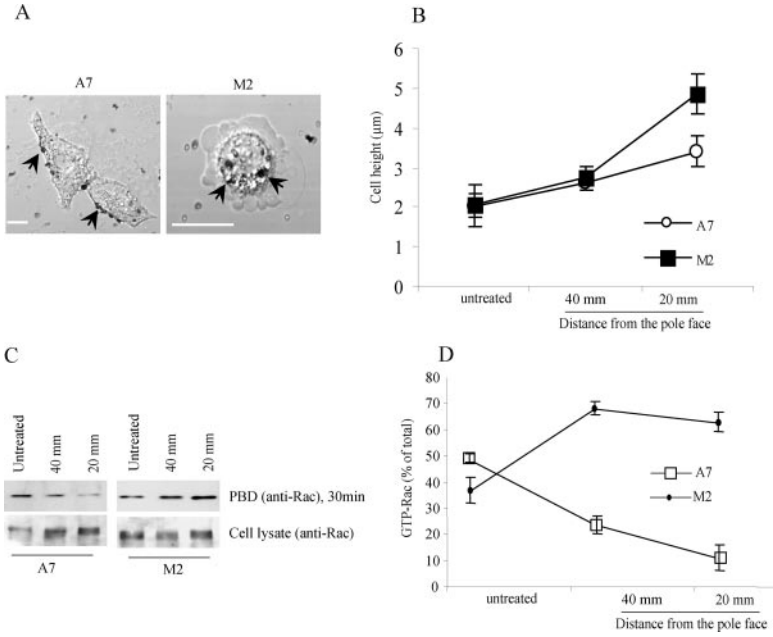

Figure 3. Force-induced cell deformation by magnetite beads. (A) A7 and M2 cells were incubated with collagen-coated magnetite beads, subjected to mechanical force by placing a permanent magnet at different distances from the culture dish surface, and analyzed by confocal microscopy. Attached beads are indicated by arrowheads. (B) Deformation of cells treated as described in A was measured using a confocal scanning laser microscope by obtaining a z-stack series of images of the untreated and force-treated cells. Cell height is calculated as the difference between the exact Z-position of the start point and the end point of the phalloidin-stained dorsal cell membrane. At least 10 cells were assessed in each sample. (C) A7 and M2 cells were treated as described in A. Cell extracts were then incubated with GST-PBD immobilized on glutathione-Sepharose beads, and the amounts of Rac in cell lysates before pull-down and GST-PBD–bound Rac were detected by immunoblot. (D) Intensities of bands were measured using ImageJ densitometry software. Numbers represent ratio relative to the levels of Rac in cell lysates before pull-down and are expressed as the means and SDs of three independent experiments. *$p <$ 0.01 versus respective untreated control.

in Rac activity comparing with untreated cells. At the same time, A7 cells exhibited a 1.6-fold increase of cell deformation and >4-fold decrease in levels of active Rac. These data suggest that, despite the possible generation of the interbead forces by aggregating magnetite beads that occurs after application of magnetic fields, the applied tensile forces are nevertheless able to deform cells. Even when we load the cells with low numbers of beads (i.e., 5–10 beads/cell) (Figure 3A), there was sufficient force applied to the cell to induce Rac activation in FLNa-deficient cells and to cause extensive cell deformation. Furthermore, lower force levels could still induce Rac activation in FLNa-deficient cells.

Force-induced FilGAP Recruitment

Our results demonstrated widely different force-induced Rac responses in FLNa-expressing and FLNa-deficient cells (Figure 4). Recent studies described a novel FLNa-binding RhoGTPase-activating protein, FilGAP. This protein suppresses Rac-mediated cell polarization in vivo, an activity that seems to be a result of targeting of FilGAP by FLNa (Ohta *et al*., 2006). Because force promotes redistribution of FLNa to the β1 integrin-collagen bead locus (Glogauer *et al*., 1998; D'Addario *et al*., 2001), we considered that force may cause changes in FilGAP distribution. We transiently transfected HEK and 3T3 cells with the full-length FilGAP construct and subjected them to force for 2 h. In FLNa-expressing cells FilGAP clearly accumulated in the subcortical region. In contrast, in FLNa-deficient FLNa-KD cells, FilGAP was equally distributed throughout the cytoplasm (Figure 4, A and B).

The interaction of FLNa with FilGAP is mediated by the coiled coil domain of FilGAP (Ohta *et al*., 2006). Accordingly, we generated a mutant FilGAP lacking the coiled-coil domain and examined whether the redistribution of FilGAP that was induced by force was affected by this truncation. HEK and 3T3 cells transfected with FilGAP$^{\Delta cc}$ demonstrated diffuse staining of FilGAP after 2 h of force, similar to that of FLNa-KD cells (Figure 4, A and B).

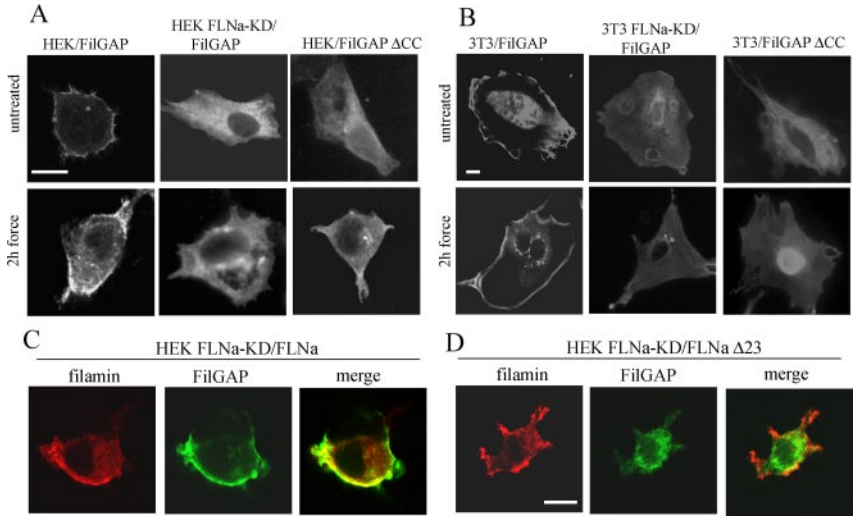

Figure 4. Force-induced redistribution of FilGAP. Wild-type and FLNa-knock down HEK (A) and wild-type and FLNa-knockdown NIH 3T3 cells (B) were plated on fibronectin-coated glass coverslips, transfected with HA-tagged FilGAP or HA-tagged FilGAP$^{\Delta CC}$ for 48 h, and then either untreated or subjected to force. FilGAP was localized by staining the cells with anti-HA antibody. (C) FLNa-knockdown HEK cells were double-transfected with HA-tagged FilGAP and DsRed-FLNa construct, incubated with collagen beads, and subjected to force. (D) Double-transfection of FLNa-knockdown HEK cells with HA-tagged FilGAP and DsRed-FLNa$^{\Delta 23}$ constructs. Transfected cells were incubated with collagen beads and subjected to force. Cellular distribution of DsRed-FLNa was directly visualized (red), whereas FilGAP was detected with anti-HA antibody (green). Bar, 10 μm.

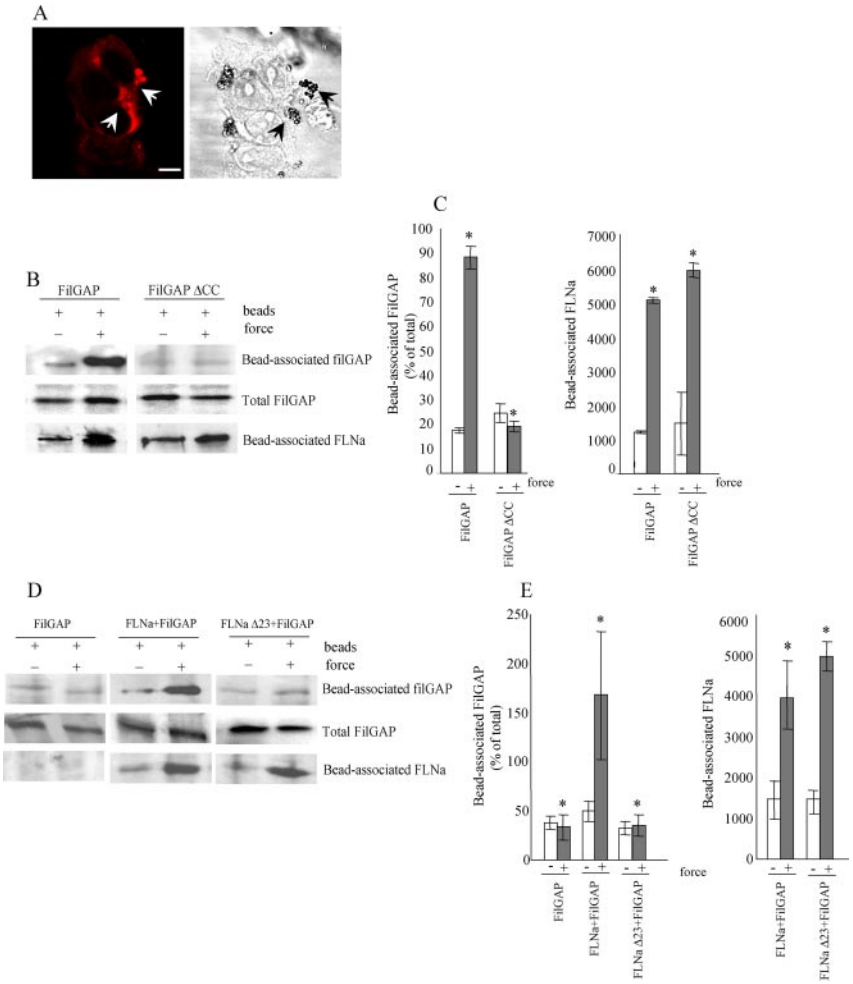

Figure 5. Recruitment of FilGAP to bead complexes. (A) HEK cells were grown on coverslips, transfected with FilGAP, and subjected to mechanical force as described in text. FilGAP was visualized by staining with anti-HA antibody. Accumulation of FilGAP in the bead complexes is indicated by arrows. (B) HEK cells, grown on 10-cm cell culture dishes, were transfected with FilGAP or FilGAP$^{\Delta CC}$ and either subjected to mechanical force as described in text or left untreated. Proteins associated with beads were obtained by bead isolation technique as described in *Materials and Methods* and analyzed by immunoblotting. (C) Quantification of bead-associated FilGAP and FLNa. Quantities of bead-associated FilGAP are represented as ratios relative to the levels of FilGAP in crude cell lysates. Bead-associated FLNa is presented by peak intensity. (D) FLNa-KD HEK cells were transfected with HA-tagged FilGAP and either full-length FLNa or truncated FLNa$^{\Delta 23}$ construct. Cells were subjected to force and bead-associated proteins were obtained as described previously. (E) Quantification of bead-associated FilGAP and FLNa was done as described in C. Intensities of all bands were measured using ImageJ densitometry software. Data are expressed as the means and SDs of three independent experiments. *$p < 0.03$ versus respective untreated control.

FilGAP bind to FLNa at the 23rd C-terminal repeat (Ohta *et al*., 2006). We assessed the role of FLNa in force-induced FilGAP redistribution by generating a truncated construct of FLNa that lacks terminal repeat 23 (FLNa$^{\Delta 23}$). HEK FLNa-KD cells were transfected with the FilGAP construct and with either full-length FLNa or FLNa$^{\Delta 23}$. In force-challenged FLNa-KD cells, restoration of full-length FLNa resulted in redistribution of FilGAP to the subcortical region (Figure 4C). In contrast, in cells transfected with FLNa$^{\Delta 23}$ mechanical force did not change the diffuse staining of FilGAP throughout the cytoplasm (Figure 4D).

We assessed the recruitment of FilGAP protein to the β1 integrin–collagen bead locus. In HEK cells subjected to mechanical force, FilGAP colocalized to bead complexes (Figure 5A). Analysis of the bead-bound proteins demonstrated that force promoted fivefold enrichment of full-length FilGAP associated with beads, whereas the levels of truncated FilGAP$^{\Delta cc}$ remained unchanged (Figure 5, B and C). Conversely, in HEK FLNa-KD cells lacking FLNa, there was no force-induced enrichment of full-length FilGAP. This outcome could be reversed by restoring the expression of full-length FLNa but not with FLNa$^{\Delta 23}$ lacking repeat 23 (Figure 5, D and E).

We found that deletion of the coiled-coli domain of FilGAP or the 23rd terminal repeat of FLNa had no effect on the previously reported (Glogauer *et al*., 1998; D'Addario *et al*., 2001) force-induced recruitment of FLNa to beads (Figure 5, B–E). We observed a >3.5-fold force-promoted enrichment of bead-associated FLNa$^{\Delta 23}$ (Figure 5, D and E), suggesting that similar to the wild-type FLNa, this mutant is fully capable of binding to β1 integrin complexes Collectively, these results suggest that in response to mechanical force, FLNa targets FilGAP to subcortical membranes and promotes its enrichment at β1 integrins bound to beads. This targeting requires the coiled-coil domain of FilGAP and the 23rd terminal repeat of FLNa.

FLNa Mediates Force-induced Lamellae Suppression by FilGAP

Because FilGAP has been shown to antagonize Rac activity in vivo, the inhibition of force-induced lamellae formation that we observed in FLNa-expressing cells may be due to FLNa mediating the activity of FilGAP. We used siRNA targeting FilGAP to reduce the expression of endogenous FilGAP in FLNa-expressing 3T3 cells (Figure 6A) and then subjected the cells to mechanical force. FITC-labeled siRNA was used to determine that >70% of cells were transfected (data not shown). Depletion of FilGAP in these cells resulted in the formation of multiple force-induced protrusions (Figure 6B) rich in cortactin (data not shown). We next evaluated Rac activation in FilGAP-depleted cells. When we subjected FilGAP-depleted 3T3 cells to 2 h of force, they exhibited a twofold increase in the levels of active Rac compared with untreated cells (Figure 6, C and D). FilGAP expression in siRNA-treated cells was restored by transfection with an HA-tagged FilGAP construct. Staining with anti-HA anti-

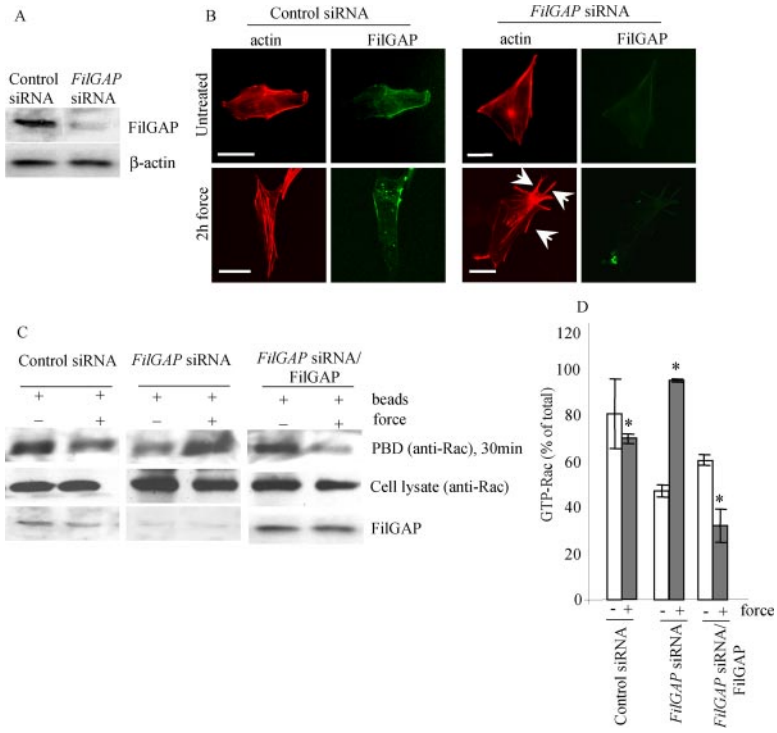

Figure 6. FilGAP suppresses force-induced lamellae. (A) Immunoblot showing that FilGAP is depleted 48 h after siRNA treatment of NIH 3T3 cells. (B) 3T3 cells were plated on fibronectin-coated glass coverslips and treated with siRNA targeting endogenous FilGAP as described in A. Cells were loaded with equal amount of collagen-coated beads and either left untreated or subjected to force. FilGAP and F-actin were localized by staining the cells with anti-FilGAP antibody (green) and rhodamine-phalloidin (red), respectively. Lamellipodia are indicated by arrows. Bar, 20 μm. (C) 3T3 cells were treated with siRNA alone as described in A or, after 48 h, they were transfected with full-length FilGAP. Cells were then subjected to force as described in B. Cell extracts were incubated with GST-PBD and immobilized on glutathione-Sepharose beads. The amount of Rac in cell lysates before pull-down; GST-PBD–bound Rac was detected by immunoblot. (D) Intensities of GST-PBD–bound Rac bands were measured using ImageJ densitometry software. Numbers represent ratios relative to the levels of Rac in cell lysates before pull-down and are expressed as the means and SDs of three independent experiments. *$p < 0.05$ versus respective untreated control.

body showed that >60% of cells were transfected (data not shown). When no force was applied, cells exhibited significant levels of active Rac. However, after 2 h of force, the levels of GTP-Rac were reduced by 1.8-fold, similar to control cells (1.2-fold decrease) (Figure 6, C and D).

The FilGAP$^{\Delta GAP}$ mutant lacking the GAP domain acts as a dominant-negative reagent, probably by sequestering upstream regulators of endogenous FilGAP (Ohta *et al.*, 2006). We transfected 3T3 cells with this mutant and subjected them to mechanical force. Force-loaded cells expressing this mutant produced 2.6 times more lamellopodia than untransfected cells (Figure 7). FilGAP$^{\Delta CC}$-expressing cells also responded to force by a 3.2-fold increase in the number of force-induced lamellae, similar to the number of force-induced lamellae in 3T3 FLNa-KD cells. The lack of the GAP domain did not affect force-induced accumulation of FilGAP$^{\Delta GAP}$ in the subcortical region of the cell or lamellipodia, whereas the lack of coiled-coil domain abolished this accumulation (Figure 7). Collectively, these results suggest that the ability of FilGAP to suppress force-induced lamellae is dependent on its coiled-coil domain and is mediated by the binding to FLNa.

FilGAP and FLNa Are Involved in Mechanoprotection

Previous studies showed that tensile forces applied through collagen receptors can induce increased apoptosis in cells and that FLNa expression protects against force-induced cell polarization and death (Kainulainen *et al.*, 2002). The relative abundance of phosphatidyl-serine in the cell membrane in early apoptotic cells can be detected by annexin-V binding (van den Eijnde *et al.*, 1997). We first tested the proapoptotic effect of different force magnitudes on FLNa-deficient and FLNa-expressing cells. Both low- and high-magnitude forces promoted only moderate increases in the percentage of annexin-V–positive and PI-negative apoptotic HEK cells (2.7-fold at 40 mm from the pole face and 4.5-fold at 20 mm from the pole face). In contrast, HEK FLN-KD cells exhibited a 15.2- and 20-fold increase in annexin staining at lower and higher force magnitudes, respectively (Figure 8).

Early stages of apoptosis involve reorganization of the actin cytoskeleton that is controlled by a wide variety of cellular proteins, including Rho family GTPases (Esteve *et al.*, 1995; Esteve *et al.*, 1998). Because FilGAP seems to suppress force-induced Rac activity, we examined whether

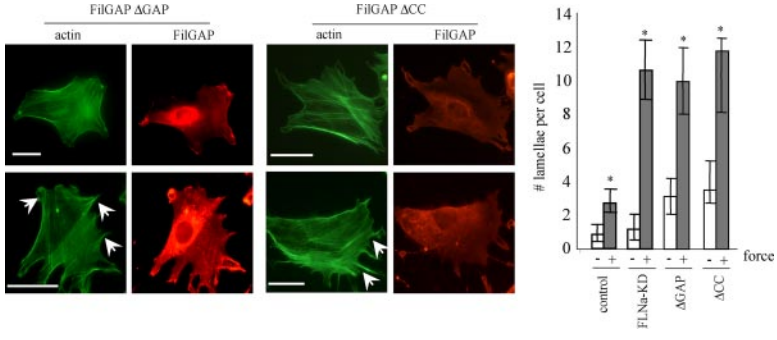

Figure 7. Requirement of FilGAP activity and binding to FLNa for suppression of force-induced lamellae. 3T3 cells were either left untransfected or transfected with HA-tagged FilGAP$^{\Delta GAP}$ (dominant negative) or FilGAP$^{\Delta CC}$, lacking coiled-coil domain. After 48 h, cells were incubated with collagen-coated beads and subjected to mechanical force or left untreated. FilGap and F-actin were visualized by staining the cells with anti-HA antibody (red) and FITC-phalloidin (green), respectively; lamellipodia are indicated with arrowheads. Bar, 20 μm. Numbers of lamellipodia were counted. The figures show means and SDs of three microscopic fields, with an average of 50 cells per each field. *$p < 0.05$ versus respective untreated control.

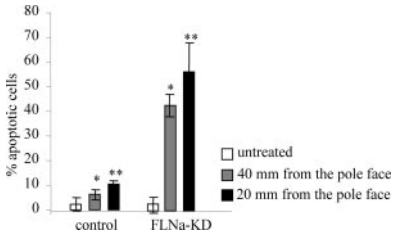

Figure 8. Force-induced apoptosis in FLNa-deficient cells. Control HEK and FLN-KD HEK cells were incubated with collagen-coated beads and either left untreated or subjected to mechanical force of different magnitude by changing the distance between the permanent magnet and the culture dish surface. Apoptotic and necrotic cells were detected with annexin-V-Fluos and PI staining, respectively. Apoptosis was measured as the percentage of annexin-V-Fluos–positive cells out of total number of cells in microscopic field and represent means and SDs of three microscopic fields, an average of 100 cells per field. *$p < 0.01$ versus respective untreated control.

force-induced recruitment of FilGAP to the cell periphery by FLNa may play a role in mechanoprotection during initial stages of apoptosis. Similar to FLNa-deficient cells, HEK cells, depleted of endogenous FilGAP by siRNA treatment, exhibited a 23.5-fold increase of apoptotic staining when subjected to 3 h of force (Figure 9, A and D). Expression of dominant-negative FilGAP$^{\Delta GAP}$ or FilGAP$^{\Delta cc}$ lacking coiled-coil domain in FilGAP-depleted HEK cells failed to rescue the phenotype. Cells transfected with these constructs exhibited levels of force-induced apoptosis similar to those of FLNa-depleted cells; in contrast, reexpression of full-length FilGAP resulted in low levels of force-induced apoptosis similar to those of control cells (Figure 9, B and D). Restoration of FLNa expression in HEK FLN-KD cells also brought the level of force-induced apoptosis to that of a control HEK cells (only a 5.8-fold increase) (Figure 9, C and D). In contrast, in HEK FLN-KD cells expressing FLNa$^{\Delta 23}$ (lacking repeat 23), there was no mechanoprotective effect (Figure 9, C and D). Together, these results suggest that FilGAP plays a role in protecting cells against early force-induced apoptosis, a function that requires interaction with FLNa.

DISCUSSION

In this study, we investigated the role of FLNa and the FLNa-binding protein FilGAP in mechanical force-induced changes of actin cytoskeletal organization. We provide evidence that FLNa suppresses force-induced lamellopodia and Rac activation by recruiting FilGAP to the β1 integrin–collagen bead locus. This specific targeting of FilGAP is mediated by interaction of its coiled-coil domain with the 23rd C-terminal repeat of FLNa and plays a role in protecting cells from force-induced apoptosis.

FLNa-deficient cells have impaired cell locomotion and exhibit circumferential blebbing of plasma membrane, which results from a relatively unstable submembrane cortex (Cunningham *et al*., 1992; Cunningham, 1995). Notably, one of the most striking differences between FLNa-deficient and FLNa-expressing cells is their response to mechanical force. We showed that cells depleted of FLNa responded to mechanical forces applied through β1 integrins by extending multiple lamellae. In contrast, in FLNa-expressing cells, force promoted formation of stress fibers. As actin stress fibers and lamellopodia formation are regulated by the small GTPases Rho and Rac, respectively (Hall, 1998), FLNa may be involved in force-induced remodeling of the actin cytoskeleton by these GTPases.

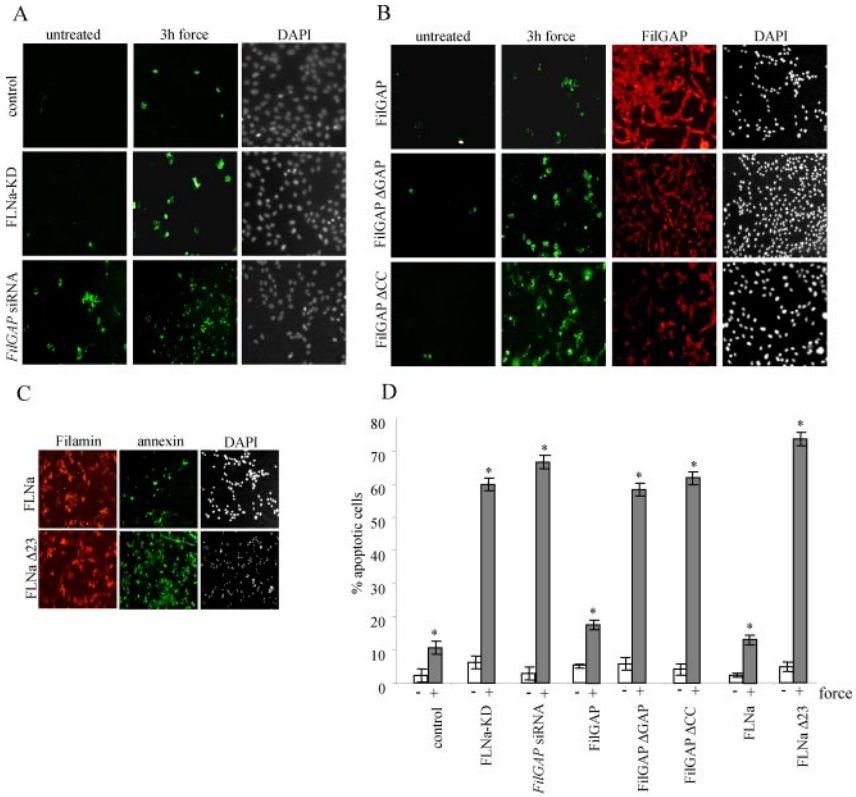

Figure 9. Inhibition of force-induced apoptosis. (A) Control HEK, FLN-KD HEK, and HEK cells pretreated with FilGAP siRNA for 48 h were incubated with collagen-coated beads and subjected to mechanical force or left untreated. Apoptotic and necrotic cells were detected with annexin-V-Fluos (green) and PI (data not shown), respectively, and the total amount of cells in each microscopic field was visualized by DAPI staining. (B) HEK cells were plated on fibronectin-coated glass coverslips and pretreated with FilGAP siRNA. Forty-eight hours later, cells were transfected with HA-tagged FilGAP, FilGAP$^{\Delta GAP}$, and FilGAP$^{\Delta CC}$ constructs. After 24 h, cells were subjected to mechanical force or left untreated, and apoptotic cells were visualized as described in A. Transfection efficiency was determined by staining the cells with anti-HA antibody (red). (C) HEK FLNa-KD cells were transfected with either full-length DsRed-FLNa or DsRed-FLNa$^{\Delta 23}$ construct, subjected to force and stained as described in A. (D) Quantification of apoptosis. For all cells apoptosis was measured as the percentage of annexin-V-Fluos–positive cells out of total number of cells in microscopic field, multiplied by transfection efficiency. Data are means and SDs of three microscopic fields, an average of 80 cells per field. *$p < 0.0002$ versus respective untreated control.

Recently, several studies reported the ability of mechanical stimuli to modulate the activity of small GTPases (Katsumi *et al*., 2002; Tzima *et al*., 2002; Smith *et al*., 2003; Wojciak-Stothard and Ridley, 2003; Kaunas *et al*., 2005; Tzima, 2006; Wu *et al*., 2007; Zhao *et al*., 2007). For example, endothelial cells initially respond to shear stress by Rho inhibition and the disassembly of existent stress fibers (Tzima *et al*., 2001; Tzima *et al*., 2002; Civelekoglu-Scholey *et al*., 2005). Simultaneously, Rac activity is transiently increased. However, prolonged exposure to shear force in these cells eventually leads to Rho activation and stress fiber reassembly, and these changes are essential for the orientation of newly formed stress fibers in the direction of applied force (Tzima *et al*., 2001; Smith *et al*., 2003; Wojciak-Stothard and Ridley, 2003; Civelekoglu-Scholey *et al*., 2005; Zhao *et al*., 2007). In contrast to endothelial cells, smooth muscle and fibroblast cells subjected to equibiaxial stretch, exhibit transient decrease in Rac activity (Katsumi *et al*., 2002). We found that in FLNa-expressing cells prolonged exposure to mechanical force applied through magnetite beads increased Rho activity and stress fiber formation together with Rac inactivation. In contrast, FLNa-deficient cells responded to prolonged force by markedly elevated levels of active Rac and multiple lamellae formation, whereas Rho activity decreased or remained unchanged. This difference in cell response was present even after exposure to lower magnitude forces (0.3 Pa), when force-induced deformation of FLNa-expressing and FLNa-deficient cells was similar. FLNa, therefore, emerges as a suppressor of force-induced Rac activation. We found that this ability of FLNa to suppress Rac activation in response to force is dependent on its C-terminal repeat 23, a region that is considered a binding site for multiple proteins involved in signal transduction and cytoskeletal reorganization, including the Rho GTPases, the Rac-, and RhoG-GEF TRIO, Pak1, ROCK, and others (Ohta *et al*., 1999; Stossel *et al*., 2001; Feng and Walsh, 2004; Nagano *et al*., 2004; Popowicz *et al*., 2006). We found that although FLNa does not require the 23rd terminal repeat for recruitment to sites of force application, this sequence is essential for the ability of FLNa to suppress force-induced lamellae formation. These data suggest that the effect of FLNa on the actin cytoskeleton that we observed may be mediated by its function as a scaffold protein. Inability of FLNa-deficient cells to recruit certain proteins that modulate the activity of small GTPases may explain increased levels of Rac activity and decreased levels of Rho activation that these cells exhibit in response to force.

In HEK FLNa-KD and 3T3 FLNa-KD cells, when FLNa levels were significantly reduced by shRNA treatment, both short and prolonged force promoted a decrease in Rho activity. Interestingly, M2 cells, which are depleted of FLNa, exhibited different dynamics of Rac and Rho activation. Although after 30 min of exposure to mechanical force there were lower levels of active Rho in M2 cells, as the duration of force increased, the levels of active Rac in these cells slightly decreased, whereas Rho activity increased. Conceivably, increased Rho activity in mechanically challenged M2 cells may be a compensatory mechanism for a complete absence of a major actin-cross-linking protein, i.e., FLNa.

To apply tensile forces to substrate-attached cells, we used collagen-coated magnetite beads that attach to the surface of cells via β1 integrin receptors. Previous studies showed that the net force applied in this method is within the range that cells such as fibroblasts are likely to encounter under physiological conditions (Glogauer and Ferrier, 1998). Notably, based on the deformations that we measured using *z*-axis confocal microscopy with these force levels, elastic moduli of ~1.2 Pa would be expected for A7 cells, which is considerably less than the 8 Pa estimated from twisting bead magnetic bead rheometry for bovine endothelial cells (Wang *et al*., 1993) or from atomic force microscopy (6 kPa; Azeloglu *et al*., 2008). Conceivably, membrane tethers are detached from the cytoskeleton under our experimental conditions, as has been observed previously using laser optical tweezers for studies of membrane deformation in fibroblasts (Titushkin and Cho 2006). The membrane deformations that we observed could account for the depolarization of fibroblasts that we have observed earlier (Kainulainen *et al*., 2002) and that may be involved in early events of force-induced apoptosis.

We found no significant difference in the surface expression levels of β1 integrins in FLNa-depleted and FLNa-expressing cells, suggesting that these cells bind collagen beads with equal strength. We also found no evidence that bead aggregation (and resultant generation of local attractive or repulsive magnetic forces in adjacent beads) would significantly prevent deformation of individual cells challenged with vertically directed forces. When very low bead loading was used (and therefore interbead forces were minimal), there was still sufficient force applied to the cell to cause marked cell deformation and therefore to model the biological phenomena under investigation. These data suggesting minimal effects of interbead forces are also in agreement with a previous report indicating that interbead forces do not affect the net magnetic vertically directed forces experienced by the cell (Glogauer and Ferrier, 1998).

One of FLNa partners is a recently discovered Rho GTPase-activating factor, FilGAP. In untreated cells, the coiled-coil domain of FilGAP binds the 23rd terminal repeat of FLNa and antagonizes Rac in vivo in response to phosphorylation by ROCK that is initiated by Rho activation (Ohta *et al*., 2006). These authors proposed that FLNa contributes to FilGAP activity by targeting it to specific cellular locations, thus making it accessible to upstream and downstream regulatory factors. We found that mechanical force caused major changes in FilGAP distribution in the cell: it specifically accumulated underneath the plasma membrane and the expression of FLNa with an intact 23rd repeat was necessary for this redistribution. The enrichment of FLNa in integrin adhesions that we observed and that has also been reported previously (Glogauer *et al*., 1998; D'Addario *et al*., 2001) coincided with fivefold increase in the levels of bead-bound FilGAP. Together, with our observation that the FLNa-binding coiled-coil domain of FilGAP and the repeat 23 of FLNa are essential for force-induced accumulation of FilGAP in the subcortical region of the cell and in the integrin/matrix loci, these data indicate that FLNa plays the major role in FilGAP recruitment to the sites of force application.

The interaction of FLNa with FilGAP emerges as a key factor in maintaining low levels of active Rac in mechanically challenged cells. The same striking cytoskeletal response to mechanical stress that we observed in FLNa-deficient cells could be initiated by depletion of FilGAP by using siRNA, expression of dominant-negative FilGAP mutant, or by interfering with FilGAP–FLNa binding. In all these cases, force promoted the formation of multiple lamellae that coincided with the increased Rac activity. Our findings are consistent with the previously published observation that activation of GAPs rather than deactivation of GEFs is most likely responsible for the down-regulation of Rac in mechanically challenged cells (Katsumi *et al*., 2002). Mechanical force applied through cell surface integrins leads to the transcriptional activation of FLNa (D'Addario *et al*., 2001). We suggest that FLNa up-regulation initiates a further feed-

forward recruitment of FilGAP to the sites of force application where it can interact with Rac.

Rac GTPases are known to play a dual role in cell growth and apoptosis, depending on cell type and the nature of extracellular signals. Constitutively active Rac protects cells from apoptosis (Joneson and Bar-Sagi, 1999; Nishida *et al*., 1999; Pervaiz *et al*., 2001; Jeong *et al*., 2002; Murga *et al*., 2002), but at the same time, overexpression of active Rac induces apoptosis in fibroblasts, neurons, and epithelial cells (Embade *et al*., 2000; Harrington *et al*., 2002). The increased lamellopodia formation and Rac activation that we observed in FLNa-deficient cells coincided with increased apoptosis induced by both lower and higher magnitude magnetically induced forces. Previous studies suggested a role for FLNa in mechanoprotection (Stossel *et al*., 2001; Kainulainen *et al*., 2002). Increased FLNa production inhibits force-induced cell death by blocking membrane depolarization (Kainulainen *et al*., 2002). We show here that FilGAP may also function as a mechanoprotective protein. Force-induced apoptosis can be markedly elevated in cells by expressing dominant-negative FilGAP construct, by depleting endogenous FilGAP by using siRNA or by interfering with the interaction of FilGAP with FLNa. Force-stimulated inhibition of Rac activity by FilGAP, which is mediated by interactions of the coiled-coil domain of FilGAP and the 23rd repeat of FLNa, thus contributes to cell survival in the face of applied tensile forces.

In conclusion, we have demonstrated that force-induced changes in the actin cytoskeleton depend on proteins associated with FLNa. FilGAP activation, which is mediated by force-induced GTP loading of Rho and specific targeting by FLNa, leads to Rac inactivation. This process in turn enhances resistance to force-induced apoptosis.

ACKNOWLEDGMENTS

We thank Thomas Stossel (Harvard Medical School) for discussions and suggestions in regard to the use of the FilGAP constructs. We also thank Wilson Lee for help with flow cytometry analyses. This work was supported by Canadian Institutes of Health Research operating (MGP-37783), group (MGC-48376), and resource grants (to C.A.M.) and by the National Institutes of Health grant R01 GM-068600 (to D.A.C.).

REFERENCES

Azeloglu, E. U., Bhattacharya, J., and Costa, K. D. (2008). Atomic force microscope elastography reveals phenotypic differences in alveolar cell stiffness. J. Appl. Physiol. *105*, 652–661.

Bellanger, J. M., Astier, C., Sardet, C., Ohta, Y., Stossel, T. P., and Debant, A. (2000). The Rac1- and RhoG-specific GEF domain of Trio targets filamin to remodel cytoskeletal actin. Nat. Cell Biol. *2*, 888–892.

Chen, C. S., Tan, J., and Tien, J. (2004). Mechanotransduction at cell-matrix and cell-cell contacts. Annu. Rev. Biomed. Eng. *6*, 275–302.

Cheng, W., Li, B., Kajstura, J., Li, P., Wolin, M. S., Sonnenblick, E. H., Hintze, T. H., Olivetti, G., and Anversa, P. (1995). Stretch-induced programmed myocyte cell death. J. Clin. Invest. *96*, 2247–2259.

Chien, S., Li, S., and Shyy, Y. J. (1998). Effects of mechanical forces on signal transduction and gene expression in endothelial cells. Hypertension *31*, 162–169.

Civelekoglu-Scholey, G., Orr, A. W., Novak, I., Meister, J. J., Schwartz, M. A., and Mogilner, A. (2005). Model of coupled transient changes of Rac, Rho, adhesions and stress fibers alignment in endothelial cells responding to shear stress. J. Theor. Biol. *232*, 569–585.

Critchley, D. R. (2000). Focal adhesions—the cytoskeletal connection. Curr. Opin. Cell Biol. *12*, 133–139.

Cunningham, C. C. (1995). Actin polymerization and intracellular solvent flow in cell surface blebbing. J. Cell Biol. *129*, 1589–1599.

Cunningham, C. C., Gorlin, J. B., Kwiatkowski, D. J., Hartwig, J. H., Janmey, P. A., Byers, H. R., and Stossel, T. P. (1992). Actin-binding protein requirement for cortical stability and efficient locomotion. Science *255*, 325–327.

D'Addario, M., Arora, P. D., Ellen, R. P., and McCulloch, C. A. (2002). Interaction of p38 and Sp1 in a mechanical force-induced, beta 1 integrin-mediated transcriptional circuit that regulates the actin-binding protein filamin-A. J. Biol. Chem. *277*, 47541–47550.

D'Addario, M., Arora, P. D., Fan, J., Ganss, B., Ellen, R. P., and McCulloch, C. A. (2001). Cytoprotection against mechanical forces delivered through beta 1 integrins requires induction of filamin A. J. Biol. Chem. *276*, 31969–31977.

Edwards, Y. S., Sutherland, L. M., and Murray, A. W. (2000). NO protects alveolar type II cells from stretch-induced apoptosis. A novel role for macrophages in the lung. Am. J. Physiol. Lung Cell Mol. Physiol. *279*, L1236–L1242.

Embade, N., Valeron, P. F., Aznar, S., Lopez-Collazo, E., and Lacal, J. C. (2000). Apoptosis induced by Rac GTPase correlates with induction of FasL and ceramides production. Mol. Biol. Cell. *11*, 4347–4358.

Esteve, P., del Peso, L., and Lacal, J. C. (1995). Induction of apoptosis by rho in NIH 3T3 cells requires two complementary signals. Ceramides function as a progression factor for apoptosis. Oncogene *11*, 2657–2665.

Esteve, P., Embade, N., Perona, R., Jimenez, B., del Peso, L., Leon, J., Arends, M., Miki, T., and Lacal, J. C. (1998). Rho-regulated signals induce apoptosis in vitro and in vivo by a p53-independent, but Bcl2 dependent pathway. Oncogene *17*, 1855–1869.

Feng, Y., and Walsh, C. A. (2004). The many faces of filamin: a versatile molecular scaffold for cell motility and signalling. Nat. Cell Biol. *6*, 1034–1038.

Glogauer, M., Arora, P., Chou, D., Janmey, P. A., Downey, G. P., and McCulloch, C. A. (1998). The role of actin-binding protein 280 in integrin-dependent mechanoprotection. J. Biol. Chem. *273*, 1689–1698.

Glogauer, M., Arora, P., Yao, G., Sokholov, I., Ferrier, J., and McCulloch, C. A. (1997). Calcium ions and tyrosine phosphorylation interact coordinately with actin to regulate cytoprotective responses to stretching. J. Cell Sci. *110*, 11–21.

Glogauer, M., and Ferrier, J. (1998). A new method for application of force to cells via ferric oxide beads. Pflugers Arch. *435*, 320–327.

Glogauer, M., Ferrier, J., and McCulloch, C. A. (1995). Magnetic fields applied to collagen-coated ferric oxide beads induce stretch-activated Ca2+ flux in fibroblasts. Am. J. Physiol. *269*, C1093–C1104.

Hall, A. (1998). Rho GTPases and the actin cytoskeleton. Science *279*, 509–514.

Harrington, A. W., Kim, J. Y., and Yoon, S. O. (2002). Activation of Rac GTPase by p75 is necessary for c-jun N-terminal kinase-mediated apoptosis. J. Neurosci. *22*, 156–166.

Huang, S., and Ingber, D. E. (1999). The structural and mechanical complexity of cell-growth control. Nat. Cell Biol. *1*, E131–E138.

Jeong, H. G., Cho, H. J., Chang, I. Y., Yoon, S. P., Jeon, Y. J., Chung, M. H., and You, H. J. (2002). Rac1 prevents cisplatin-induced apoptosis through down-regulation of p38 activation in NIH3T3 cells. FEBS Lett. *518*, 129–134.

Joneson, T., and Bar-Sagi, D. (1999). Suppression of Ras-induced apoptosis by the Rac GTPase. Mol. Cell. Biol. *19*, 5892–5901.

Kainulainen, T., Pender, A., D'Addario, M., Feng, Y., Lekic, P., and McCulloch, C. A. (2002). Cell death and mechanoprotection by filamin a in connective tissues after challenge by applied tensile forces. J. Biol. Chem. *277*, 21998–22009.

Katsumi, A., Milanini, J., Kiosses, W. B., del Pozo, M. A., Kaunas, R., Chien, S., Hahn, K. M., and Schwartz, M. A. (2002). Effects of cell tension on the small GTPase Rac. J. Cell Biol. *158*, 153–164.

Katsumi, A., Orr, A. W., Tzima, E., and Schwartz, M. A. (2004). Integrins in mechanotransduction. J. Biol. Chem. *279*, 12001–12004.

Kaunas, R., Nguyen, P., Usami, S., and Chien, S. (2005). Cooperative effects of Rho and mechanical stretch on stress fiber organization. Proc. Natl. Acad. Sci. USA *102*, 15895–15900.

Kiema, T., Lad, Y., Jiang, P., Oxley, C. L., Baldassarre, M., Wegener, K. L., Campbell, I. D., Ylänne, J., and Calderwood, D. A. (2006). The molecular basis of filamin binding to integrins and competition with talin. Mol. Cell *21*, 337–347.

Kobayashi, Y., Hashimoto, F., Miyamoto, H., Kanaoka, K., Miyazaki-Kawashita, Y., Nakashima, T., Shibata, M., Kobayashi, K., Kato, Y., and Sakai, H. (2000). Force-induced osteoclast apoptosis in vivo is accompanied by elevation in transforming growth factor beta and osteoprotegerin expression. J. Bone Miner. Res. *15*, 1924–1934.

Lin, P. M., Chen, C. T., and Torzilli, P. A. (2004). Increased stromelysin-1 (MMP-3), proteoglycan degradation (3B3- and 7D4) and collagen damage in cyclically load-injured articular cartilage. Osteoarthr. Cartil. *12*, 485–496.

Lionetti, V., Recchia, F. A., and Ranieri, V. M. (2005). Overview of ventilator-induced lung injury mechanisms. Curr. Opin. Crit. Care *11*, 82–86.

Malek, A. M., and Izumo, S. 1996. Mechanism of endothelial cell shape change and cytoskeletal remodeling in response to fluid shear stress. J. Cell Sci. *109*, 713–726.

Makarova, O., Kamberov, E., and Margolis, B. (2000). Generation of deletion and point mutations with one primer in a single cloning step. Biotechniques *29*, 970–972.

Marti, A., Luo, Z., Cunningham, C., Ohta, Y., Hartwig, J., Stossel, T. P., Kyriakis, J. M., and Avruch, J. (1997). Actin-binding protein-280 binds the stress-activated protein kinase (SAPK) activator SEK-1 and is required for tumor necrosis factor-alpha activation of SAPK in melanoma cells. J. Biol. Chem. *272*, 2620–2628.

McNeil, P. L., and Steinhardt, R. A. (1997). Loss, restoration, and maintenance of plasma membrane integrity. J. Cell Biol. *137*, 1–4.

Meng, X., Yuan, Y., Maestas, A., and Shen, Z. (2004). Recovery from DNA damage-induced G2 arrest requires actin-binding protein filamin-A/actin-binding protein 280. J. Biol. Chem. *279*, 6098–6105.

Murga, C., Zohar, M., Teramoto, H., and Gutkind, J. S. (2002). Rac1 and RhoG promote cell survival by the activation of PI3K and Akt, independently of their ability to stimulate JNK and NF-kappaB. Oncogene *21*, 207–216.

Nagano, T., Morikubo, S., and Sato, M. (2004). Filamin A and FILIP (Filamin A-Interacting Protein) regulate cell polarity and motility in neocortical subventricular and intermediate zones during radial migration. J. Neurosci. *24*, 9648–9657.

Nishida, K., Kaziro, Y., and Satoh, T. (1999). Anti-apoptotic function of Rac in hematopoietic cells. Oncogene *18*, 407–415.

Ohta, Y., Hartwig, J. H., and Stossel, T. P. (2006). FilGAP, a Rho- and ROCK-regulated GAP for Rac binds filamin A to control actin remodelling. Nat. Cell Biol. *8*, 803–814.

Ohta, Y., Suzuki, N., Nakamura, S., Hartwig, J. H., and Stossel, T. P. (1999). The small GTPase RalA targets filamin to induce filopodia. Proc. Natl. Acad. Sci. USA *96*, 2122–2128.

Pervaiz, S., Cao, J., Chao, O. S., Chin, Y. Y., and Clement, M. V. (2001). Activation of the RacGTPase inhibits apoptosis in human tumor cells. Oncogene *20*, 6263–6268.

Pi, M., Spurney, R. F., Tu, Q., Hinson, T., and Quarles, L. D. (2002). Calcium-sensing receptor activation of rho involves filamin and rho-guanine nucleotide exchange factor. Endocrinology *143*, 3830–3838.

Plopper, G., and Ingber, D. E. (1993). Rapid induction and isolation of focal adhesion complexes. Biochem. Biophys. Res. Commun. *193*, 571–578.

Popowicz, G. M., Schleicher, M., Noegel, A. A., and Holak, T. A. (2006). Filamins: promiscuous organizers of the cytoskeleton. Trends Biochem. Sci. *31*, 411–419.

Sadoshima, J., and Izumo, S. (1997). The cellular and molecular response of cardiac myocytes to mechanical stress. Annu. Rev. Physiol. *59*, 551–571.

Shyy, J. Y., and Chien, S. (1997). Role of integrins in cellular responses to mechanical stress and adhesion. Curr. Opin. Cell Biol. *9*, 707–713.

Smith, P. G., Roy, C., Zhang, Y. N., and Chauduri, S. (2003). Mechanical stress increases RhoA activation in airway smooth muscle cells. Am. J. Respir. Cell. Mol. Biol. *28*, 436–442.

Stossel, T. P., Condeelis, J., Cooley, L., Hartwig, J. H., Noegel, A., Schleicher, M., and Shapiro, S. S. (2001). Filamins as integrators of cell mechanics and signalling. Nat. Rev. Mol. Cell Biol. *2*, 138–145.

Takai, Y., Sasaki, T., and Matozaki, T. (2001). Small GTP-binding proteins. Physiol. Rev. *81*, 153–208.

Thubrikar, M. J., and Robicsek, F. (1995). Pressure-induced arterial wall stress and atherosclerosis. Ann. Thorac. Surg. *59*, 1594–1603.

Titushkin, I., and Cho, M. (2006). Distinct membrane mechanical properties of human mesenchymal stem cells determined using laser optical tweezers. Biophys. J. *90*, 2582–2591.

Tzima, E. (2006). Role of small GTPases in endothelial cytoskeletal dynamics and the shear stress response. Circ. Res. *98*, 176–185.

Tzima, E., Del Pozo, M. A., Kiosses, W. B., Mohamed, S. A., Li, S., Chien, S., and Schwartz, M. A. (2002). Activation of Rac1 by shear stress in endothelial cells mediates both cytoskeletal reorganization and effects on gene expression. EMBO J. *21*, 6791–6800.

Tzima, E., del Pozo, M. A., Shattil, S. J., Chien, S., and Schwartz, M. A. (2001). Activation of integrins in endothelial cells by fluid shear stress mediates Rho-dependent cytoskeletal alignment. EMBO J. *20*, 4639–4647.

Ueda, K., Ohta, Y., and Hosoya, H. (2003). The carboxy-terminal pleckstrin homology domain of ROCK interacts with filamin-A. Biochem. Biophys. Res. Commun. *301*, 886–890.

Vadlamudi, R. K., Li, F., Adam, L., Nguyen, D., Ohta, Y., Stossel, T. P., and Kumar, R. (2002). Filamin is essential in actin cytoskeletal assembly mediated by p21-activated kinase 1. Nat. Cell Biol. *4*, 681–690.

van den Eijnde, S. M., Luijsterburg, A. J., Boshart, L., De Zeeuw, C. I., van Dierendonck, J. H., Reutelingsperger, C. P., and Vermeij-Keers, C. (1997). In situ detection of apoptosis during embryogenesis with annexin V: from whole mount to ultrastructure. Cytometry *29*, 313–320.

van der Flier, A., and Sonnenberg, A. (2001). Structural and functional aspects of filamins. Biochim. Biophys. Acta *1538*, 99–117.

Wang, N., Butler, J. P., and Ingber, D. E. (1993). Mechanotransduction across the cell surface and through the cytoskeleton. Science *260*, 1124–1127.

Weaver, A. M., Karginov, A. V., Kinley, A. W., Weed, S. A., Li, Y., Parsons, J. T., and Cooper, J. A. (2001). Cortactin promotes and stabilizes Arp2/3-induced actin filament network formation. Curr. Biol. *11*, 370–374.

Weed, S. A., and Parsons, J. T. (2001). Cortactin: coupling membrane dynamics to cortical actin assembly. Oncogene *20*, 6418–6434.

Wennerberg, K., Rossman, K. L., and Der, C. J. (2005). The Ras superfamily at a glance. J. Cell Sci. *118*, 843–846.

Wojciak-Stothard, B., and Ridley, A. J. (2003). Shear stress-induced endothelial cell polarization is mediated by Rho and Rac but not Cdc42 or PI 3-kinases. J. Cell Biol. *161*, 429–439.

Wu, C. C., Li, Y. S., Haga, J. H., Kaunas, R., Chiu, J. J., Su, F. C., Usami, S., and Chien, S. (2007). Directional shear flow and Rho activation prevent the endothelial cell apoptosis induced by micropatterned anisotropic geometry. Proc. Natl. Acad. Sci. USA *104*, 1254–1259.

Zhao, X. H., Laschinger, C., Arora, P., Szaszi, K., Kapus, A., and McCulloch, C. A. (2007). Force activates smooth muscle alpha-actin promoter activity through the Rho signaling pathway. J. Cell Sci. *120*, 1801–1809.